Geomorphology 322 (2018) 41–52

Contents lists available at ScienceDirect

Geomorphology

journal homepage: www.elsevier.com/locate/geomorph

Sediment load responses to climate variation and cascade reservoirs in the Yangtze River: A case study of the Jinsha River

Dongfeng Li [a], Xi Xi Lu [a,b,*], Xiankun Yang [c], Li Chen [d], Lin Lin [a]

[a] Department of Geography, National University of Singapore, Kent Ridge 117570, Singapore
[b] Inner Mongolian Key Lab of River and Lake Ecology, School of Ecology and Environment, University of Inner Mongolia, Hohhot 010021, China
[c] School of Geographical Sciences, Guangzhou University, Guangzhou 510006, China
[d] State Key Laboratory of Water Resources and Hydropower Engineering Science, Wuhan University, Wuhan 430072, China

ARTICLE INFO

Article history:
Received 11 March 2018
Received in revised form 29 August 2018
Accepted 29 August 2018
Available online 31 August 2018

Keywords:
Jinsha River
Sediment load
Discharge
Climate change
Cascade reservoirs
Three Gorges Reservoir

ABSTRACT

Climate change and human activities have substantially changed hydrological and geomorphologic processes, particularly in upper mountainous catchments. The Jinsha River Basin (JRB), the uppermost region of the Yangtze River and the largest hydropower production region in China, was chosen to investigate the sediment load responses to climate variations and human activities. The non-parametric Mann-Kendall test and double mass curve were used to explore the spatial-temporal variations of hydro-meteorological variables and quantify the contributions of climate variation and human activities to changes in discharge and sediment load in the JRB from the 1950s to 2015. The results indicate that human activities, in particular cascade damming, were the governing factor for sediment load changes, while climate variations (increasing precipitation and snow and glacier melt) dominated the discharge changes in the JRB. The average annual sediment load at the Panzhihua (PZH) station increased by 42.4% from 1966–1984 to 1985–2010, mainly due to mineral extraction and deforestation, followed by a decrease of 75.9% in 2011–2015 because of the operation of the cascade reservoirs in the middle JRB since 2010. The construction of new dams like the Xiangjiaba Reservoir (2012) and the Xiluodu Reservoir (2013) in the lower JRB and many other cascade reservoirs since 2010 in the middle JRB further decreased the sediment load by 58.5% (BHT) and 83.8% (XJB) in the recent five years from 2011 to 2015. Although channel erosion downstream of the XJB Dam can provide new sediment to the Three Gorges Reservoir (TGR), the sedimentation rate of the TGR has decreased rapidly and will continue to be reduced due to the construction of more dams in the future.

© 2018 Elsevier B.V. All rights reserved.

1. Introduction

Rivers, as conveyor belts between land and ocean, have annually transported approximate 36,000 km^3 of freshwater and >20 Gt of sediment and other terrestrial materials into the global oceans (Milliman and Farnsworth, 2011; Yang et al., 2014). The transport of water, sediment and other materials can significantly affect fluvial processes, delta evolutions as well as riverine and coastal biogeochemical processes (Syvitski et al., 2005; Walling, 2006; Wang et al., 2008; Latrubesse et al., 2017). Global climate change in recent decades has resulted in rapid changes of hydrological cycle in snow-dominated and rainfall-dominated zones in both local and regional scales (Barnett et al., 2005; Yang and Lu, 2015). In particular, the amounts and intensities of precipitation are increasing (e.g., more extreme rainfall events), which have triggered more frequent floods and yielded more sediment load in many rivers of the world (Allen and Ingram, 2002; Nearing et al., 2005; Li et al., 2016).

In addition to climate change, human activities, such as damming, land use change as well as industrial activities, have been widely reported to profoundly influence discharge and sediment load (Syvitski et al., 2005; Milliman et al., 2008). Damming has been considered as the most paramount reason for sediment load reduction in rivers all over the world (Chakraborti, 2005). It also disrupts the continuity of the sediment transport in river systems and causes substantial changes in annual and seasonal flow and sediment regimes (Wang et al., 2008). In contrast, land use change (deforestation in particular) and industrial activities such as road construction and mineral extraction can accelerate soil erosion and increase sediment yield (Higgitt and Lu, 1999).

Recently, hydrological responses to climate change and human activities have received increasing attention from researchers worldwide (Miao et al., 2011; Naik and Jay, 2011; Liu et al., 2014). However, most studies have concentrated on separating the impact of climatic and human factors on discharge or streamflow (Lu et al., 2013; Zhao

* Corresponding author at: Department of Geography, National University of Singapore, Kent Ridge 117570, Singapore.
E-mail address: geoluxx@nus.edu.sg (X.X. Lu).

https://doi.org/10.1016/j.geomorph.2018.08.038
0169-555X/© 2018 Elsevier B.V. All rights reserved.

et al., 2017), and few studies have been conducted to the quantitative assessments of the impact of climate change and human activities on sediment load particularly in high mountainous rivers around the world. Therefore, separating impact of climatic and human factors on both sediment load and discharge in the uppermost reaches is necessary for sustainable management of river ecology of the whole basin. For example, a detailed study of upstream sediment load changes is needed for a better management of downstream reservoirs.

The Jinsha River Basin (JRB), located in the uppermost region of the Yangtze River, is one of the most important sediment sources for the Yangtze River and the largest hydropower production region in China. The source of the JRB is the Qinghai-Tibet Plateau, which is widely known as the "Third Pole" and "Water Tower of Asia". Global warming has accelerated the glacier retreat and permafrost degradation on the plateau (Lutz et al., 2014). Human activities such as damming, deforestation, agriculture and industry disturbances have been intensified in this region since the 1950s. In particular, four mega reservoirs (Wudongde (WDD), Baihetan (BHT), Xiluodu (XLD), Xiangjiaba (XJB)) in the lower Jinsha River and eight mega reservoirs in the middle Jinsha River will be or have been constructed in recent years (Fig. 1). The four mega cascade reservoirs in the lower JRB have an installed hydropower generation capacity of 40×10^8 kW (twice the capacity of the Three Gorges Reservoir (TGR)) and a total storage capacity of 410×10^8 m^3 (larger than that of the TGR's, 393×10^8 m^3). These cascade reservoirs will further change the annual and seasonal flow and sediment regimes and even affect the operation of the TGR.

Climatic data and hydrological data in the JRB will be used to quantitatively assess the impact of climate change and human activities on discharge and sediment load in the JRB. The objectives of this study are to (1) detect the trends and abrupt change points in annual discharge and sediment load; (2) quantify the individual impact of climate change and human activities on discharge and sediment load variability; and (3) explore the impact of sediment load changes in the upper reaches on the TGR's sedimentation.

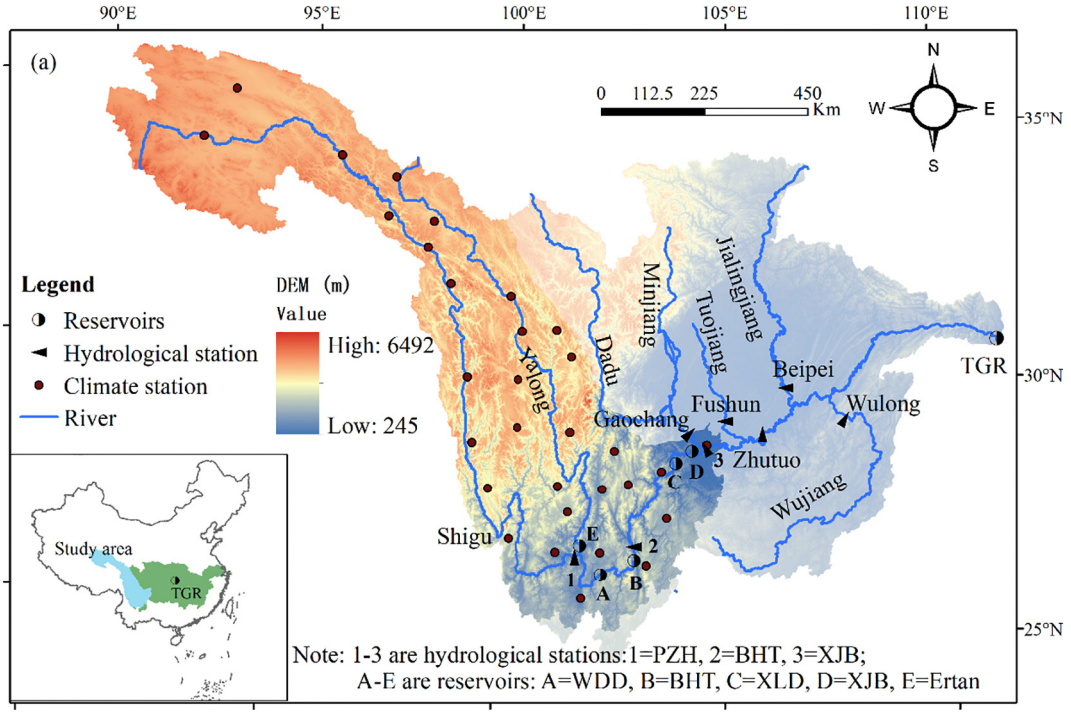

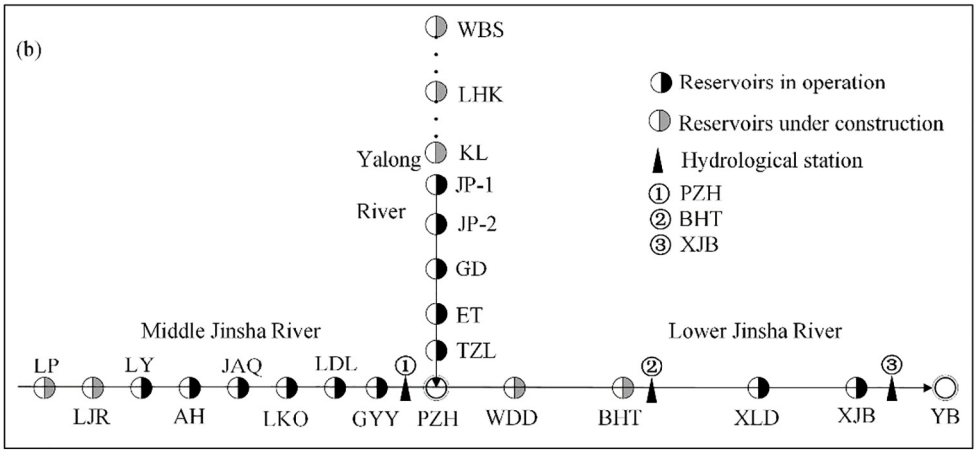

Fig. 1. Location of the study area (a) and the distribution of the hydrological stations and cascade reservoirs in the middle-lower Jinsha River and the Yalong River (b). PZH = Panzhihua, BHT = Baihetan, XJB = Xiangjiaba.

2. Study area and data

2.1. Study site

The JRB includes the Jinsha River and its largest tributary Yalong River (Fig. 1(a)) and covers four provinces (Qinghai, Xizang, Yunnan and Sichuan) with an area of approximate 500,000 km^2, accounting for 27.8% of the Yangtze River basin. The Jinsha River, with an elevation fall of 5000 m from the Qinghai-Tibet Plateau to the Sichuan Basin, can be divided into three parts: the upper part (from Yushu to Shigu), the middle part (from Shigu to Panzhihua) and the lower part (from Panzhihua to Yibin). The high Tibet Plateau lies in an arid zone, while the middle-lower reaches of the basin lie in a wet climate zone, dominated by the Indian monsoon (Higgitt and Lu, 1999). The spatial and temporal distribution of precipitation within the basin shows significant heterogeneity. The average annual precipitation ranges from 300 mm (at the uppermost reach and the lower dry-hot valley area) to 1200 mm. The rainfall in the wet season constitutes 90% of the total annual precipitation.

The JRB provides annually approximate 38% of discharge (~140 billion m^3) and 57% of sediment load (~230 million t) to the Upper Yangtze River. Therefore, the JRB is the main source of sediment in the Upper Yangtze (Higgitt and Lu, 1999). Many mega cascade reservoirs have recently been built or are under construction in the middle-lower JRB, with the four representatives in the lower mainstream (WDD, BHT, XLD and XJB), eight cascades (Longpan, Liangjiaren, Liyuan, Ahai, Jinanqiao, Longkaikou, Ludila and Guanyinyan) in the middle mainstream and five typical reservoirs (Jinping-1, Jinping-2, Guandi, Ertan and TZL) in the tributary of the Yalong River (Fig. 1(b)). Given these recent developments in the JRB, there is an urgent need to quantitatively assess the changes of discharge and sediment load caused by both climate change and human activities.

2.2. Data

Data in this study consists of the annual temperature, precipitation, discharge and sediment load in the JRB from the 1950s to 2015. Daily precipitation and temperature data for the 30 meteorological stations plotted in Fig. 1 were retrieved from the National Climate Center of China Meteorological Administration (http://data.cma.gov.cn). The meteorological data were preprocessed with quality control by removing data that deviated considerably from historical records and by interpolating missing data with the data from neighboring stations or time series. The catchment-averaged precipitation and temperature for sub-basins were calculated by the Thiessen polygon method (Thiessen, 1911) with the assumption that meteorological stations are evenly distributed in each sub-basin. Annual discharge and sediment load data at the Panzhihua (PZH, 1966–2015), Baihetan (BHT, 1952–2015), and Xiangjiaba (XJB, 1954–2015) stations were provided by the Changjiang Water Resources Commission (CWRC) and the *Bulletin of Yangtze River Sediment* (http://www.cjh.com.cn). In addition, the daily discharge and sediment load data at the XJB station (1954–2007) were collected and converted to monthly values for seasonal assessments in the JRB.

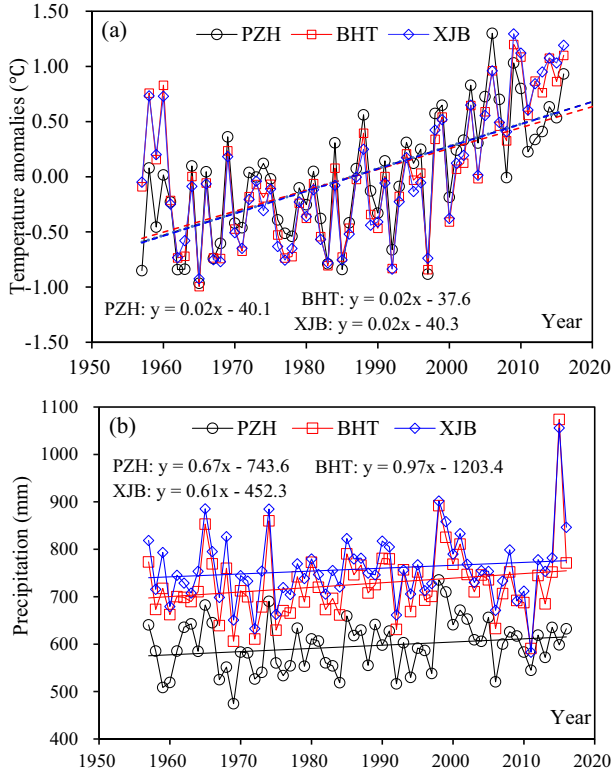

Fig. 2. Annual trends for the temperature anomalies (a) and precipitation (b) in the JRB. Temperature anomalies and precipitation were analyzed using catchment-averaged data.

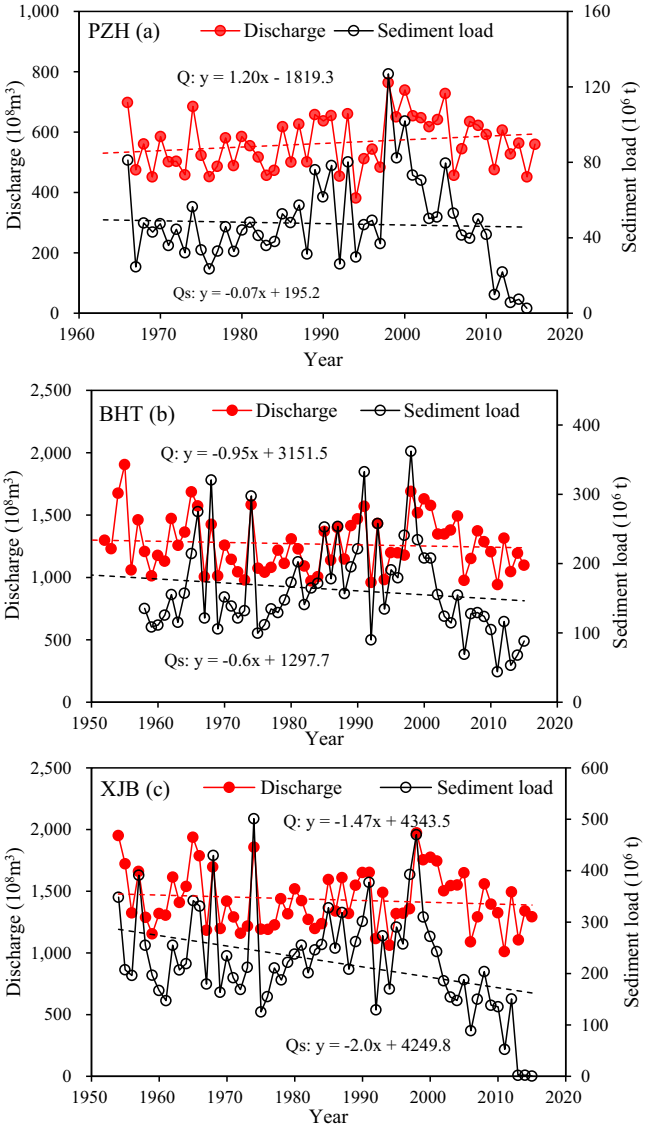

Fig. 3. Temporal variations for the annual discharge (Q) and sediment load (Q_S) at the PZH (a), BHT (b) and XJB (c) stations.

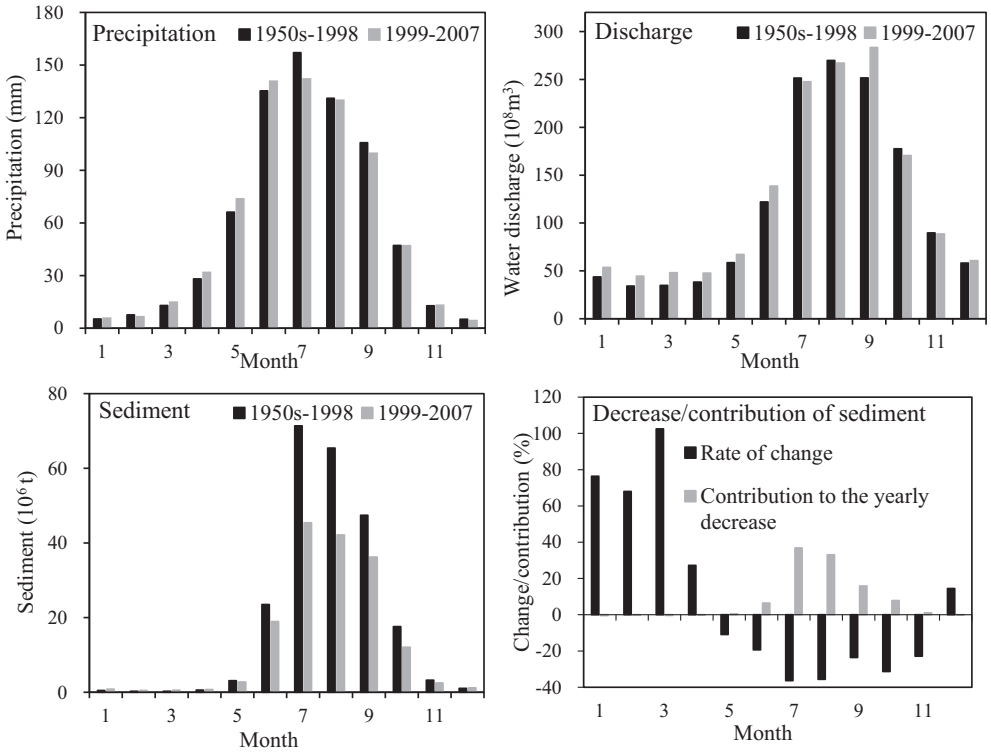

Fig. 4. Seasonal changes of precipitation, discharge and sediment load before and after 1999 at the XJB station.

3. Methods

3.1. Trend analysis

The rank-based, non-parametric Mann-Kendall (M-K) test (Mann, 1945; Kendall, 1975) is widely used to assess the monotonic trends and abrupt change points of environmental time series, especially for hydroclimatic time series (Zhang and Lu, 2009; Miao et al., 2011). This method has been firmly established due to its robust statistics. In this study, the M-K test was used to detect the trends of hydroclimatic variables such as temperature (T), precipitation (P), discharge (Q) and sediment load (Q_S).

The null hypothesis H_0 is that no significant trend occurs for an independent and identically distributed time series $\{X = X_1, X_2, \ldots, X_n\}$. The alternative hypothesis H_1 is that the monotonic occurs in X. The statistic S is defined as:

$$S = \sum_{i=1}^{n-1} \sum_{j=j+1}^{n} \mathrm{sgn}(x_j - x_i) \tag{1}$$

where n is the number of data points, and x_i and x_j are the data values in time series i and j ($j > i$), respectively. In Eq. (1), $\mathrm{sgn}(x_j - x_i)$ is the sign function, which is given by

$$\mathrm{sgn}(x_j - x_i) = \begin{cases} 1 & x_j > x_i \\ 0 & x_j = x_i \\ -1 & x_j < x_i \end{cases} \tag{2}$$

Mann (1945) and Kendall (1975) stated that when n ≥ 8, the statistic S is approximately normally distributed with the following variance:

$$Var(S) = \frac{n(n-1)(2n+5) - \sum_{p=1}^{q} t_p (p-1)(2p+5)}{18} \tag{3}$$

in which n = the number of data points, q is the number of tied groups, and t_p denotes the number of ties of size p. The standardized test statistic Z is computed using Eq. (4):

$$Z = \begin{cases} \dfrac{S-1}{\sqrt{\mathrm{var}(S)}} & S>0 \\ 0 & S = 0 \\ \dfrac{S+1}{\sqrt{\mathrm{var}(S)}} & S<0 \end{cases} \tag{4}$$

in Eq. (4), Z is the test statistic. Positive Z values indicate increasing trends, whereas negative Z values indicate decreasing trends. The null hypothesis of no trend (H_0) is rejected at the significance level of α if $|Z| > Z_{(1-\alpha/2)}$, where α is the significance level of the test and $Z_{(1-\alpha/2)}$ is the critical value of the standard normal distribution with a probability exceeding $\alpha/2$. Since the M–K test was used in this study to detect whether the

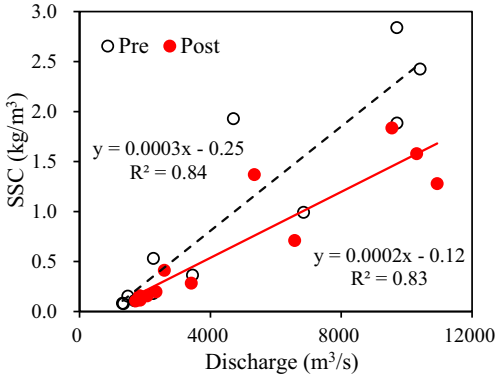

Fig. 5. Correlations between the monthly average SSC and discharge in the pre- and post-change periods at the XJB station. Pre = 1957–1998; Post = 1999–2007.

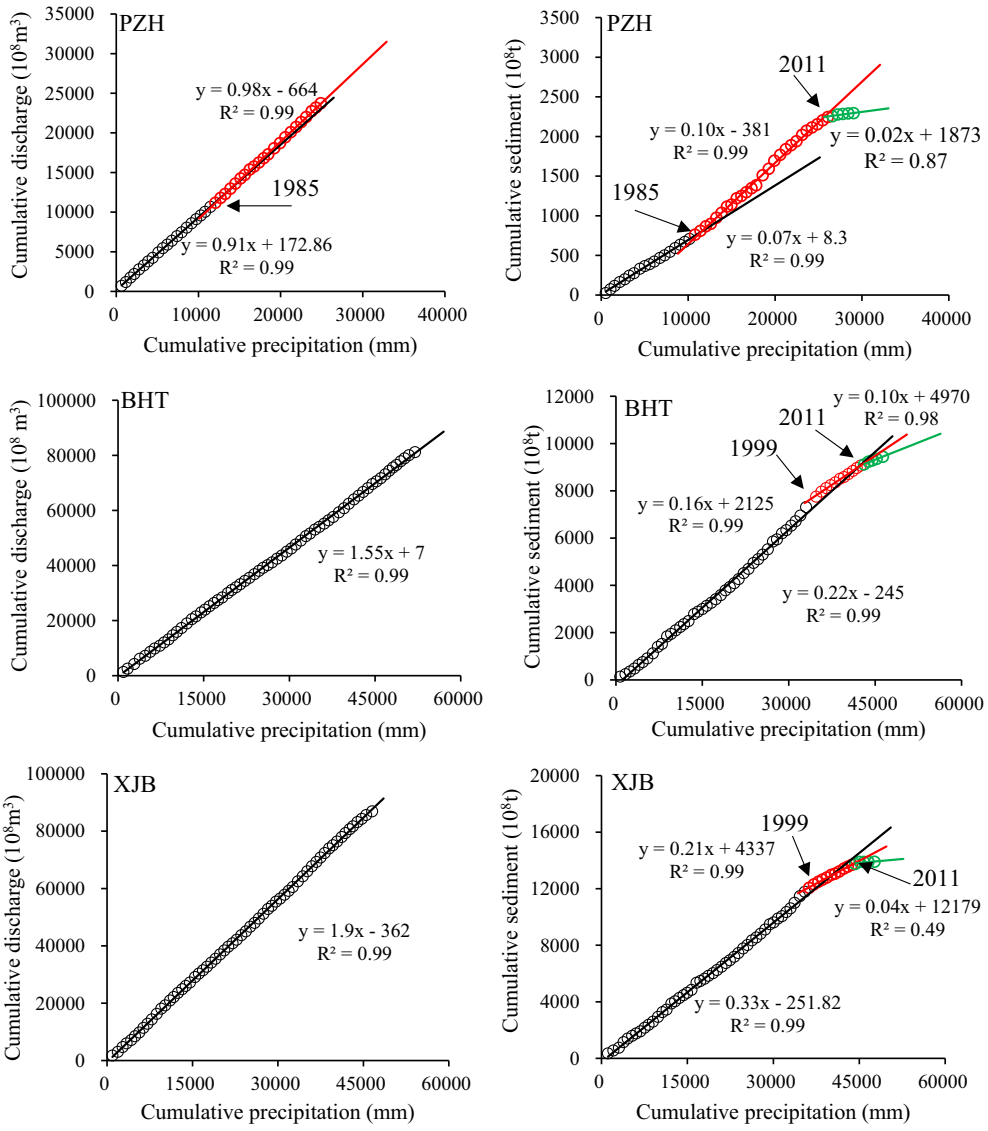

Fig. 6. Double mass curves of cumulative precipitation vs. cumulative discharge and sediment load. The straight lines are the linear regression lines for the data in the pre- and post-change periods.

regression is statistically significant, hydro-climatic variables trends were also determined through the simple linear regression.

3.2. Abrupt change analysis

The M-K test method was also used to detect the occurrence of a change point in discharge and sediment load. For a given time series $\{X = X_1, X_2, \ldots, X_n\}$, the M-K rank statistic (S_k) is calculated as (Mann, 1945):

$$S_k = \sum_{i=1}^{k} r_i \quad (2 \le k \le n) \tag{5}$$

$$r_i = \begin{cases} 1 & x_j \ge x_i \\ 0 & x_j \ge x_i \end{cases} \quad (j = 1, 2, 3, \ldots, i) \tag{6}$$

The mean and variance of the test statistic (S_k) are calculated as:

$$E[S_k] = \frac{n(n-1)}{4} \tag{7}$$

$$Var[S_k] = \frac{n(n-1)(2n+5)}{72} \tag{8}$$

The sequential values of the statistic UF_k are then calculated as:

$$UF_K = \frac{S_K - E[S_K]}{Var[S_K]} \tag{9}$$

UF_k is normally distributed and constitutes a forward sequence curve. Following the same procedure, the retrograde time series $\{X = X_n, X_{n-1}, \ldots, X_1\}$ was used to calculate the backward sequence of the statistic $UB_k = -UF_k$ ($k = n, n-1, \ldots, 1$). Hence, the sequential version of this test is exhibited in a graphical format, showing curves of the statistics UF_k and UB_k. The UF_k statistic displays the time evolution of the analyzed series, and the UB_k is plotted to determine the beginning of the change. If the intersection of the two lines UF_k and UB_k is within the confidence interval, a change point is seen to have occurred.

To ensure the accuracy of the statistical detection, the cumulative anomaly method (Ran et al., 2010) was also used to test the abrupt change points for discharge and sediment load in the JRB (Zhao et al., 2015).

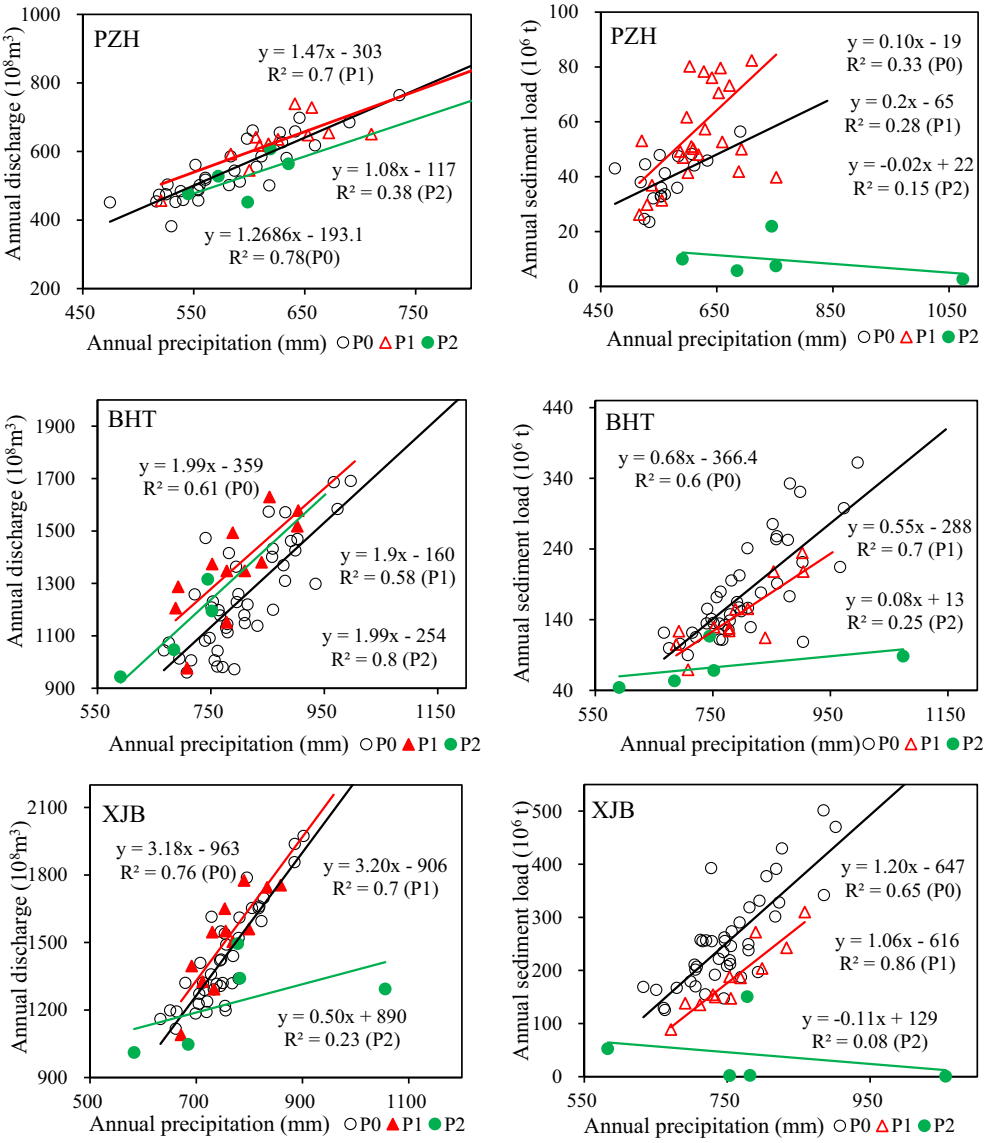
PZH
y = 1.47x - 303
R² = 0.7 (P1)
y = 1.08x - 117
R² = 0.38 (P2)
y = 1.2686x - 193.1
R² = 0.78(P0)
Annual discharge (10⁸m³)
Annual precipitation (mm) ○P0 △P1 ●P2
PZH
y = 0.10x - 19
R² = 0.33 (P0)
y = 0.2x - 65
R² = 0.28 (P1)
y = -0.02x + 22
R² = 0.15 (P2)
Annual sediment load (10⁶ t)
Annual precipitation (mm) ○P0 △P1 ●P2
BHT
y = 1.99x - 359
R² = 0.61 (P0)
y = 1.9x - 160
R² = 0.58 (P1)
y = 1.99x - 254
R² = 0.8 (P2)
Annual discharge (10⁸m³)
Annual precipitation (mm) ○P0 ▲P1 ●P2
BHT
y = 0.68x - 366.4
R² = 0.6 (P0)
y = 0.55x - 288
R² = 0.7 (P1)
y = 0.08x + 13
R² = 0.25 (P2)
Annual sediment load (10⁶ t)
Annual precipitation (mm) ○P0 △P1 ●P2
XJB
y = 3.18x - 963
R² = 0.76 (P0)
y = 3.20x - 906
R² = 0.7 (P1)
y = 0.50x + 890
R² = 0.23 (P2)
Annual discharge (10⁸m³)
Annual precipitation (mm) ○P0 ▲P1 ●P2
XJB
y = 1.20x - 647
R² = 0.65 (P0)
y = 1.06x - 616
R² = 0.86 (P1)
y = -0.11x + 129
R² = 0.08 (P2)
Annual sediment load (10⁶ t)
Annual precipitation (mm) ○P0 △P1 ●P2

Fig. 7. Correlations between annual precipitation and discharge, annual precipitation and sediment load in the JRB. For the PZH station: P0 = 1950s–1984; P1 = 1985–2010; P2 = 2011–2015; For the BHT and XJB: P0 = 1950s–1998; P1 = 1999–2010; P2 = 2011–2015.

3.3. Double curve method

Several methods, most notably the double mass curve, sediment identity approach, and sediment yield models, have been developed to separate the impacts of climate variation and human activities on sediment load (Zhao et al., 2018). Among these methods, the double mass curve method has been most widely used to quantify the contributions of climate change and human activities on discharge and sediment load, particularly for a large-scale basin (Restrepo and Syvitski, 2006; Walling, 2006; Zhao et al., 2018). A double mass curve is a plot of the cumulated values of one variable against another related variable in a concurrent period. A straight line will be plotted if the two cumulated variables show constant proportionality, whereas the inflection of the curve presents a change of the constant proportionality.

In this study, double mass curves of cumulative precipitation vs. cumulative discharge or sediment load were plotted in the pre- and post-change period based on the abrupt change analysis. Subsequently, linear regression equations were calculated based on the two cumulative variables in the pre-change period. Taking the sediment load as an example, the predicted sediment load in the post-change period (S_{postc}) can be obtained by extrapolating the established linear regression equations. The change in sediment load can be calculated as:

$$\Delta S = S_{posto} - S_{preo} \tag{10}$$

where ΔS is the change in sediment load, S_{posto} is the observed sediment in the post-change period, and S_{preo} is the observed sediment in the pre-change period.

The sediment load change caused by the climate variability and human activity in the post-change period can be calculated by:

$$S_{cli} = S_{postc} - S_{preo} \tag{11}$$

where S_{cli} denotes the mean annual sediment load changes due to climate change.

$$S_{hum} = \Delta S - S_{cli} \tag{12}$$

where S_{hum} denotes the mean annual sediment load changes due to human activities.

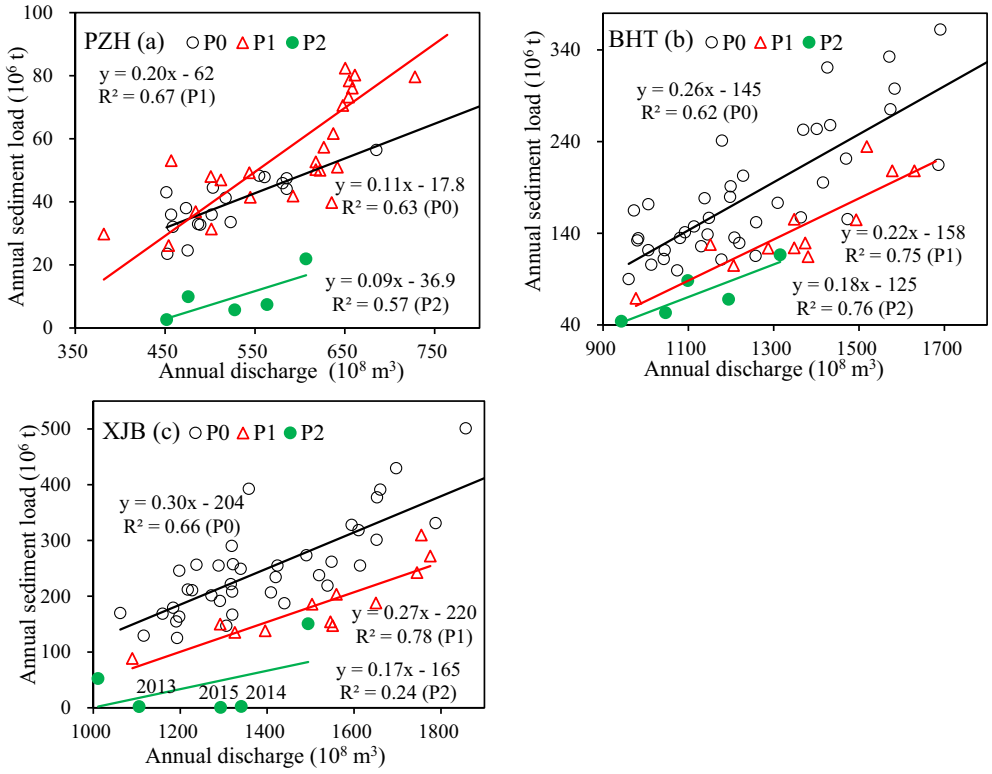

Fig. 8. Correlations between the annual sediment load and the annual discharge in the JRB.

4. Results

4.1. Trends of hydro-climate variables

Table 2 and Fig. 2 show the mean annual temperature, precipitation, discharge and sediment load in the JRB since the 1950s as ascertained by the MK test and linear regression methods. Overall, the annual average temperature from 1957 to 2015 in the three catchments displayed a significant increasing trend, with a decadal rising rate of 0.2 °C. This warming trend is consistent with the IPCC report (2014) and previous findings in the Yangtze Basin (Lu et al., 2013). The precipitation exhibited a positive trend in the JRB with increase rates of 0.67, 0.97 and 0.61 mm yr^{-1} at the PZH, BHT, and XJB stations, respectively, although this trend was not statistically significant (Table 2).

The discharge showed no significant trend in the JRB although a moderate increase (1.2×10^8 m^3 yr^{-1}) was observed at the PZH station (Fig. 3). The rising trend at the PZH was consistent with the annual precipitation changes. The slight declines in discharge at the BHT and XJB stations are not comparable to the precipitation variations, which were likely caused by the increased evapotranspiration due to the rising temperature (Table 2) and by soil and water conservation practices (Zhou et al., 2008; Zhao et al., 2014). However, in general, these findings indicate that there were no remarkable runoff changes in the Yangtze basin, which is in line with previous studies (Zhao et al., 2015).

The sediment load exhibited a decreasing trend in the whole JRB with a significant reduction rate of 2×10^6 t yr^{-1} at the XJB station and slighter reduction rates of 0.6×10^6 t yr^{-1} and 0.07×10^6 t yr^{-1} at the BHT and PZH station, respectively (Fig. 3). The average annual

Table 1
Basic information of the cascade reservoirs in the JRB.

	Reservoirs	Operation time	Storage capacity (10^8 m^3)	Watershed area (10^4 km^2)	Installed capacity (10^4 kW)
Middle	Longpan (LP)	–	371	21.4	420
Jinsha River	Liangjiaren (LJR)	–	74.2	21.84	320
	Liyuan (LY)	2014.11	7.27	22	240
	Ahai (AH)	2011.12	8.06	23.54	200
	Jinanqiao (JAQ)	2010.10	9.13	23.74	240
	Longkaikou (LKK)	2012.11	5.58	24	180
	Ludila (LDL)	2013.4	17.18	24.73	216
	Guanyinyan (GYY)	2014.10	0.72	25.65	300
Lower	Wudongde (WDD)	–	74	40.61	870
Jinsha River	Baihetan (BHT)	–	206	43.03	1350
	Xiluodu (XLD)	2013.5	126.7	45.4	1386
	Xiangjiaba (XJB)	2012.10	115.7	45.9	640
Yalong River	Jinping-1 (JP-1)	2013	77.6	10.26	360
	Jinping-2 (JP-2)	2012	0.14	10.3	480
	Guandi (GD)	2012	7.6	11	240
	Ertan (ET)	1999	58	11.64	330
	Tongzilin (TZL)	2014	0.91	12.85	60

Note: – indicates reservoirs under construction.

Table 2
Spatial and temporal trends for the annual temperature, precipitation, discharge and sediment load in the JRB using the Mann-Kendall test.

Stations	Temperature		Precipitation		Discharge		Sediment load	
	Z	*P*	*Z*	*P*	*Z*	*P*	*Z*	*P*
PZH	4.28	**0**	1.51	0.131	1.23	0.219	0	1
BHT	2.4	**0.016**	1.43	0.153	−0.31	0.756	−0.9	0.368
XJB	2.3	**0.02**	0.85	0.395	−0.33	0.74	−2.41	**0.016**

Bold number of *P* indicates significant trends at 95% confidence level.

decline rates were equivalent to 0.9% (XJB), 0.35% (BHT) and 0.15% (PZH) of their mean annual sediment load. The significant reduction in sediment load was probably in response to the human activities such as damming and the implementation of soil and water conservation practices (Lu and Higgitt, 1998; Zhao et al., 2017).

4.2. Abrupt changes in discharge and sediment load

The MK change point test and cumulative anomaly methods were applied to identify the abrupt change point in annual discharge and sediment load. Table 3 shows the years in which there were abrupt changes for the discharge and sediment in the JRB. Abrupt changes for discharge at the PZH station occurred in 1985. The average annual discharge increased from 528×10^8 m^3 over the period of 1966–1985 to 586×10^8 m^3 over the period of 1986–2015. In contrast, no significant abrupt change for discharge was detected at the BHT and XJB stations.

As for the sediment load, the abrupt change point at the PZH station was also 1985. The sediment load increased around 21% after 1985 at the PZH, which may have been caused by increased precipitation and intensified human activities such as mineral extraction and deforestation (Lu et al., 2010). For the BHT and XJB stations, the two methods yielded different results of abrupt change points: 2011 by the MK and 1999 by the cumulative anomaly method, respectively. The change point of 2011 was caused by the operation of the XJB reservoir (total storage capacity: 126.7×10^8 m^3) since October 2012, the XLD reservoir (total storage capacity: 115.7×10^8 m^3) since May 2013 and the many other reservoirs upstream of the BHT. The change point of 1999 may be largely attributed to the operation of the Ertan Reservoir (total storage capacity: 58×10^8 m^3) since 1999 (Lu et al., 2010). The sediment load decreased around 34% and 48% during 1999–2010 and further decreased 57% and 83% during 2011–2015 at the BHT and XJB stations, respectively (Table 3).

4.3. Seasonal changes of precipitation, discharge and sediment load

To further understand the seasonal changes of hydro-meteorological variables in the JRB, the monthly average precipitation, discharge and sediment load at the XJB station were analyzed. Fig. 4 presents the changes in the monthly average precipitation, discharge and sediment load in the periods before and after the abrupt change year for sediment load. The wet season (from May to October) accounted for around 90% of the annual total precipitation and discharge in both pre- and post-change periods. This is mainly attributed to the Indian monsoon from the southwest, which leads to large amounts of rainfall during the warmest months of the year in the Upper Yangtze River (Wang et al., 2008). No significant changes in monthly precipitation from the pre-change to the post-change period were observed in the JRB. However, the monthly discharge in the dry season slightly increased, due to the operation of reservoirs (e.g., the Ertan Reservoir) in the JRB (Lu, 2005; Zhang et al., 2012b).

The monthly sediment load also exhibited a seasonal pattern in both pre- and post-change periods with around 95% of the annual sediment occurred during the wet season in the JRB (Fig. 4). The result is in line with previous studies in the Yangtze River basin (Liu et al., 2014; Zhao et al., 2015). However, there was also a significant decline in the monthly sediment load in the wet season after 1999 (Fig. 4). The sediment load in the dry season showed a slight increase although its contribution to the total annual sediment load was <5%. Sharp reduction in sediment load during the wet season was also caused by the operation of the reservoirs in spite of the dam-outlets for sediment sluicing (Zhang et al., 2012b). Since the sediment load decreased much more than the discharge in the post-change period (Fig. 4), the relationship between discharge and suspended sediment concentration (SSC) has been altered (Fig. 5). The reduction in SSC increased with the rising discharge, resulting in the sharp reduction in sediment load during the wet season.

4.4. Contributions of climate change and human activities to discharge and sediment load

To quantify the contributions of climate variation and human activities to discharge and sediment load changes, double mass curves and regression lines of cumulative annual precipitation (P) compared to cumulative discharge (Q) and sediment load (Q_s) in the JRB were analyzed (Fig. 6). The slope for the P-Q increased after the year of abrupt change (1985) at the PZH station. In contrast, both the BHT and XJB stations showed no change points for the discharge.

Double mass curves for the P-Q_s at the PZH, BHT, and XJB all showed abrupt changes. The slopes at the PZH increased significantly after 1985 and then decreased significantly after 2011. In contrast, the slopes at the BHT and XJB decreased slightly after 1999 and then decreased significantly after 2011, indicating reduction in sediment load in the two post-change periods (Fig. 6). The results align well with the finding of the abrupt change analysis using the MK test and cumulative anomaly methods, suggesting that sediment load changes were much more significant than discharge changes in the JRB.

The contributions of precipitation variations and human activities are summarized in Table 4a and 4b. Human activities played a dominant role in sediment load changes in the whole JRB, with the contributions of 82%, 86.6% and 89.2% in the first post-change period (P1) and 107.5%, 91.3% and 102.3% in the second post-change period (P2) at the PZH, BHT, and XJB stations, respectively. As for the discharge, precipitation contributed 53.3% to the increase at the PZH.

Table 3
Results of the abrupt changes for the annual discharge and sediment load in the JRB using the MK test and the cumulative anomaly methods.

Stations	Q				Q_S			
	Change point	Q-pre (10^8 m^3)	Q-post (10^8 m^3)	ΔQ (%)	Change point	Q_S-pre (10^6 t)	Q_S-post (10^6 t)	ΔQ_S (%)
PZH	1985(MK) 1985(CA)	528	586	10.8	1985(MK) 1985(CA)	42	51	21
BHT	–				2011(MK)	171	74	−57
	–				1999(CA)	180	118	−34
XJB	–				2011(MK)	240	41	−83
	–				1999(CA)	253	132	−48

MK = Mann-Kendall test, CA = Cumulative anomaly method, –: not significant change point; Q-pre (Q_S-pre) = average annual discharge (sediment load) before the change point, Q-post (Q_S-post) = average annual discharge (sediment load) after the change point.

Table 4a
Quantification of the impact of climate change and human activities on discharge in the JRB.

	Period	Precipitation (mm)	Q_o	Q_{postc}	ΔQ	ΔQ_{cli}	$\Delta Q_{hum+others}$
PZH	Pre-1985	568.7	528.4				
	1985–2015	610	585.7	559	57.2 (11%)	30.5 (53.3%)	26.7 (46.7%)

Q_o is the observed discharge (10^8 m^3). Data in brackets indicate the contributions of climate change or human activities to the total change.

5. Discussion

5.1. Impact of climate variation on discharge and sediment load

Climate variation (e.g., changes in temperature and precipitation) can affect discharge and sediment load (Nearing et al., 2005; Zhao et al., 2015). For instance, a warming trend can increase glacier melting and discharge. Higher precipitation will also increase discharge and sediment load (Miao et al., 2011; Naik and Jay, 2011). Therefore, the rise in temperature and precipitation (Fig. 2) in the JRB was associated with the increase in discharge at the PZH station (Fig. 3). Furthermore, the annual discharge had a significant correlation with the annual precipitation in the whole JRB (Fig. 7), which was particularly pronounced at the baseline period (P0) ($R^2 = 0.6–0.78$, $p < 0.01$).

Previous studies have documented that the relative contribution of precipitation to changes in discharge varied in different rivers. For instance, in rivers like the Yangtze basin (Zhao et al., 2017), the US Midwest rivers (Xu et al., 2013) and the Xijiang basin (Zhang and Lu, 2009), discharge changes were mainly resulted from precipitation variation. In contrast, in rivers such as the middle reaches of the Yellow River (Zhao et al., 2014), Chaobai River (Wang et al., 2009), Tarim River (Tao et al., 2011), human activities played a major role in discharge changes. In our study, a rise in discharge has been found at the PZH station since 1985 (Fig. 6) and the contribution of precipitation was 53.3% (Table 4a). The remaining contribution can be partly attributed to snow and glacier melt and human activities (e.g., deforestation results in a decrease in soil infiltration (Zhang et al., 2012a). The significant rise in temperature in this area (Table 2 and Fig. 2) could accelerate the melting of glaciers and increase discharge (Kehrwald et al., 2008; Lutz et al., 2014). For instance, when compared with the period from 1961 to 1990, the glaciers melt from 1991 to 2004 contributed around two thirds to the increase in discharge at the Tuotuohe station (Zhang et al., 2008).

The annual sediment load also showed significant correlations with the annual precipitation in the whole JRB, although the coefficients (R^2) were relatively lower than those between precipitation and discharge (Fig. 7). Previous studies (Lu et al., 2013; Zhao et al., 2015) showed that the contributions of precipitation to sediment load changes ranged from 42–61% in semi-arid rivers (the Yellow River and the Haihe River) to 0.4–11% in humid rivers (the Pearl River and the Yangtze River). The contributions in our study ranged from −2.3% to 18%, which is consistent with the previous studies of humid rivers.

The relationship between annual discharge and annual sediment load also changed (Fig. 8). From the baseline period to the post-change period, the annual sediment load decreased sharply with the same discharge, particularly in 2013, 2014, and 2015 at the XJB station (Fig. 8(c)), which was mainly caused by the operation of the mega XLD and XJB reservoirs (Table 1).

5.2. Impact of human activities on sediment load

An increased discharge at the PZH station and no significant discharge changes at the BHT and XJB stations were observed in our study (Table 3). Human activities such as water diversion, industrial (domestic) water withdrawal as well as reservoir construction can exert substantial influences on discharge changes (Naik and Jay, 2011). However, these impacts can be offset by climate variabilities such as precipitation and glacier melting (Lutz et al., 2014).

5.2.1. Damming

Damming is considered to be the most effective measure to trap and reduce sediment load from land to ocean (Chakraborti, 2005; Kummu et al., 2010; Latrubesse et al., 2017). In the JRB, significant reduction in the average annual sediment load after 1999 at the BHT and XJB stations (Table 3 and Table 4b) were closely associated with the Ertan Reservoir constructed in 1999 with a total storage capacity of 58×10^8 m^3 (Table 1). Previous studies also reported that the Ertan Reservoir could trap 90% of the annual sediment from the Yalong River, equivalent to around 20% of the annual sediment in the XJB station (Lu et al., 2010).

Table 4b
Quantification of the impact of climate change and human activities on sediment load in the JRB.

Stations	Period	Precipitation (mm)	S_o	S_{postc}	ΔS	ΔS_{cli}	ΔS_{hum}
PZH	Pre-1985 (P0)	569.4	39.3				
	1985–2010 (P1)	612.5	59.1	42.9	19.8 (42.4%)	3.6 (18%)	16.2 (82%)
	2011–2015 (P2)	594.1	9.5	41.6	−29.8 (−75.9%)	2.3 (−7.5%)	−32.1 (107.5%)
BHT	Pre-1999 (P0)	807.5	178.3				
	1999–2010 (P1)	791	146.2	174	−32.2 (−18%)	−4.3 (13.4%)	−27.9 (86.6%)
	2011–2015 (P2)	769.2	74	169.2	104.4 (−58.5%)	−9.1 (8.7%)	−95.3 (91.3%)
XJB	Pre-1999 (P0)	771.8	256.1				
	1999–2010 (P1)	748.8	173.3	247.1	−82.7 (−32%)	−8.9 (10.8%)	−73.8 (89.2%)
	2011–2015 (P2)	790.6	41.5	260.9	−214.5 (−83.8%)	4.8 (−2.3%)	−219.4 (102.3%)

S_o is the observed sediment load (10^6 t). Data in brackets indicate the contributions of climate change or human activities to the total change; "+" means a positive impact on the total change, while "−" presents a negative impact on the total change. P0 is the baseline period and P1 (P2) is the post-change period.

Table 5
Sediment deposition of the cascade reservoirs in the middle-lower JRB (Zhu et al., 2016) and the estimated reservoir trapping efficiency according to Brune (1953) and Brown (1944).

	Reservoirs	2013		2014		Brune	Brown
		Sediment deposition (10^6 t)	Measured trapping efficiency	Sediment deposition (10^6 t)	Measured trapping efficiency	Trapping efficiency	Trapping efficiency
Middle Jinsha River	Ahai + Jinanqiao	15.26	74.4%	22.3	62.7%	61.5%	43%
	Longkaikou + Ludila	–	–	5.87	44.1%	61%	46%
Lower Jinsha River	XLD			61.91	90.7%	83%	85%
	XJB			4.18	65.4%	82%	84%

Table 6
Sediment load in the upper Yangtze River including the mainstream, tributaries and TGR's sedimentation rate since 2003.

	Period	Sediment load ($\times 10^6$ t)								
		XJB	Gao chang	Fu shun	Zhu tuo	Bei pei	Wu long	TGR input	TGR output	TGR sedimentation
Average annual	2003–2015	108.7	25.2	4.8	138.8	28.7	5.0	172.6	39.3	133.3
	2003–2012	140.9	29.1	2.1	168.0	29.2	5.7	202.9	46.4	156.5
	2013–2015	1.6	12.3	13.7	41.4	27.2	2.9	71.4	15.9	55.5
Yearly	2013	2.0	20.8	36.0	68.3	57.6	0.9	126.8	32.8	94.0
	2014	2.2	11.9	3.2	34.6	14.5	6.3	55.4	10.5	44.9
	2015	0.6	4.3	1.9	21.2	9.5	1.3	32.0	4.3	27.7

Gaochang, Fushun, Beipei and Wulong are the tributary controlling stations of Minjiang, Tuojiang, Jialingjiang and Wujiang River, respectively (Fig. 1(a)). TGR input is the sum of sediment load at the stations of (Zhutuo + Beipei + Wulong), while the TGR output is the sediment load at the Huanglingmiao station (7 km downstream of the TGR).

In addition to the Ertan Reservoir, the "Changzhi" natural forest conservation project which was implemented in 1989 in the lower JRB has also contributed to the sediment reduction (Lu et al., 2010).

The average annual sediment load from 2013 to 2015 at the PZH and XJB stations was only 2.56×10^6 t and 1.6×10^6 t respectively, constituting <10% and 1% of the previous average annual sediment load (48.4×10^6 t from 1966 to 2012 at the PZH and 231.7×10^6 t from 1954 to 2012 at the XJB). This significant sediment reduction was caused by the operation of the XLD Reservoir constructed in May 2013 with a total storage capacity of 126.7×10^8 m^3 and the XJB Reservoir constructed in October 2012 with a total storage capacity of 115.7×10^8 m^3 in the lower Jinsha and other reservoirs operated since 2010 in the middle JRB (Table 1). The estimated trapping efficiencies and the huge amount of sediment deposition within these cascade reservoirs can explain the sediment load reduction in the JRB (Table 5). Another two mega reservoirs, the WDD Reservoir (total storage capacity: 74×10^8 m^3, 2020) and the BHT Reservoir (total storage capacity: 206×10^8 m^3, 2022) are being constructed (Table 1), which are expected to further reduce the sediment load in the JRB.

5.2.2. Other human activities

In addition to damming, other human activities such as deforestation, farming and industrial activities, have also been shown to substantially influence sediment load changes (Meade and Moody, 2009). In our study, the average annual sediment load at the PZH station increased 42.4% during 1985–2010 (Table 3) and 82% of this increase can be attributed to human activities other than damming. Previous studies also suggested that the sediment increase mainly resulted from human activities such as mineral extraction and deforestation since the 1980s in the JRB (Lu et al., 2010). Likewise, the sediment load at the BHT and XJB stations also increased slightly from 1985 to 1999 (Fig. 9) due to deforestation, road construction and frequent tectonic activities (landslides and debris flow) in this area (Xiong et al., 2009).

5.3. Implication for the TGR's sedimentation

Previous studies have discussed and predicted the sedimentation of the TGR (Xu and Milliman, 2009; Yang and Lu, 2014). However, the observed sedimentation in the TGR since 2003 was much less than predicted. Specifically, the average annual sedimentation for the TGR from 2003 to 2015 was 123.4×10^6 t (Table 6), only accounting for around 40% of the predicted (1961–1970s prediction scenario, Zhu et al., 2016). The sediment load in the JRB (XJB station) was positively correlated with the TGR's sediment input and sedimentation (Fig. 10). Therefore, the TGR's sedimentation was strongly influenced by the sediment load from the JRB. In particular, the reduction in sediment supply due to the cascade reservoirs in the JRB played a significant role in reducing TGR's sediment input and reservoir sedimentation after 2012. The average annual sediment load at the XJB station and TGR's sediment input decreased by 139.3×10^6 t yr^{-1} and 131.5×10^6 t yr^{-1} from 2003–2012 to 2013–2015. The two declines were largely caused by the operation of the XJB Reservoir and the XLD Reservoir. Similarly, the average annual TGR's sedimentation rate in the period of 2013–2015 decreased by 101×10^6 t yr^{-1} (65%) compared with that in the period of 2003–2012. Sediment load in the JRB will likely continue to decrease due to more mega reservoirs under construction like the WDD Reservoir and the BHT Reservoir, which will further reduce the TGR's sedimentation rate.

The SSC and sediment load decreased significantly, particularly in flood discharges after 1999 at the XJB (Fig. 4 and Fig. 5). The decreased SSC in the post-change period also reflects a decrease in sediment transport capacity of high discharge and the phenomenon of "hungry flow" or "starving flow" (Yang et al., 2007; Yuan et al., 2012), which can promote river channel incision (Chen et al., 2010). It was estimated that 22.24×10^6 m^3 (equivalent to 36.7×10^6 t, Table 7) of the riverbed sediment load were scoured from 2008 to 2015 between the XJB Dam and Yibin (29.8 km) largely due to the upstream damming, although some of the scouring may have been caused by sand extraction.

Table 7
River channel scouring volumes from the XJB Dam to Yibin (29.8 km) calculated by the field cross-sectional profiles (Zhu et al., 2016). (Negative value indicates channel erosion, while positive value indicates deposition).

Time period	Scouring volume (10^6 m^3)	Sediment load (10^6 t)
2008.3–2012.10	−13.88	−22.9
2012.10–2013.11	−3.32	−5.47
2013.11–2014.10	−4.1	−6.76
2014.10–2015.10	−0.96	−1.58
Total (2008.3–2015.10)	−22.3	−36.7

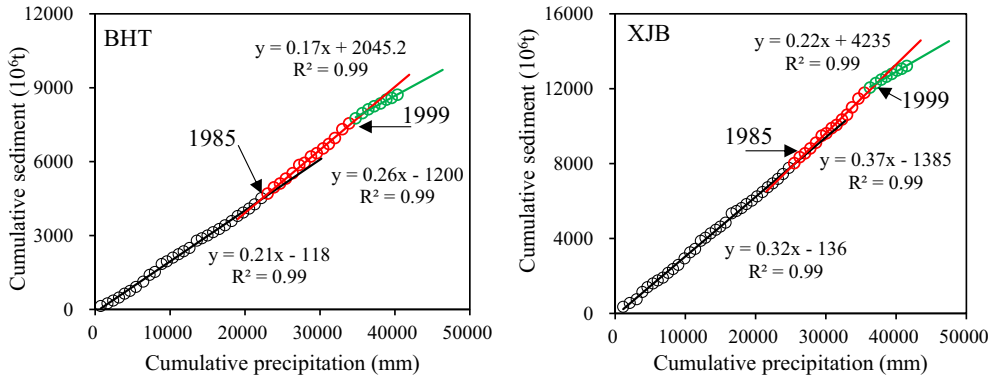

Fig. 9. Correlations between cumulative sediment and cumulative precipitation in different periods at the BHT and XJB stations, showing the rise in sediment during 1985–1999.

6. Conclusions

The results of our study indicate that human activities, in particular cascade damming, played a predominant role in sediment load changes, while climate variations mainly impacted discharge changes in the Jinsha River Basin (JRB). The average annual sediment load decreased by 18% and 32% during the period of 1999–2010 at the Baihetan (BHT) and Xiangjiaba (XJB) stations mainly due to the Ertan Reservoir in the Yalong River. The average annual sediment load decreased by 58.5% (Baihetan station) and 83.8% (Xiangjiaba station) during 2011–2015 because of the Xiluodu Reservoir (2013) and the Xiangjiaba Reservoir (2012) in the lower Jinsha River and many other cascade reservoirs constructed since 2010 in the middle Jinsha River. In contrast to the monotonic reduction of the sediment load at the Baihetan and Xiangjiaba stations, the sediment load at the Panzhihua (PZH) station increased 42.4% from 1966–1984 to 1985–2010 and then decreased 75.9% during 2011–2015. The increase in sediment load was likely the result of mineral extraction and deforestation, while the reduction during 2011–2015 was mainly caused by the operation of upstream cascade reservoirs since 2010. In addition to the sediment load changes, the discharge at the PZH station increased 11% during 1985–2015, largely due to the increased precipitation.

In response to the operation of the upstream reservoirs, significant reduction of sediment load in the wet season and a slight increase of discharge in the dry season were observed. The significant reduction in sediment load due to the mega cascade reservoirs in the Jinsha River played a dominant role in reducing the TGR's sedimentation rate, although channel erosion downstream the Xiangjiaba station provided new sediment to the TGR.

Acknowledgements

This study was supported by the National Natural Science Foundation of China (Grant No. 91547110), the National University of Singapore (Humanity and Social Sciences, Grant No. R-109-000-172-646 and NUS Research Scholarship) and the Institute of Water Policy, NUS (R-603-000-212-490). We are particularly grateful to the anonymous referees and Professor Chen Zhongyuan for their constructive comments and suggestions on the earlier version of this paper. We also thank Dr. Anneliese Kramer Dahl for helping to revise the language of this paper.

References

Allen, M.R., Ingram, W.J., 2002. Constraints on future changes in climate and the hydrologic cycle. Nature 419 (6903), 224–232.
Barnett, T.P., Adam, J.C., Lettenmaier, D.P., 2005. Potential impacts of a warming climate on water availability in snow-dominated regions. Nature 438 (7066), 303–309.
Brown, C.B., 1944. Discussion of sedimentation in reservoirs. In: Witzig, B.J. (Ed.), Transactions of the American. Society of Civil Engineers, pp. 1493–1500.
Brune, G.M., 1953. Trap efficiency of reservoirs. EOS Trans. Am. Geophys. Union 34 (3), 407–418.
Chakraborti, N., 2005. Fragmentation and flow regulation of the world's large river systems. Science 308 (5720), 405.
Chen, Z., Wang, Z., Finlayson, B., Chen, J., Yin, D., 2010. Implications of flow control by the Three Gorges Dam on sediment and channel dynamics of the middle Yangtze (Changjiang) River, China. Geology 38 (11), 1043–1046.
Higgitt, D.L., Lu, X.X., 1999. Challenges in relating land use to sediment yield in the Upper Yangtze. Hydrobiologia 410, 269–277.
IPCC, 2014. Climate change 2014: synthesis report. Contribution of Working Groups I, II and III to the Fifth Assessment Report of the Intergovernmental Panel on Climate Change. IPCC.
Kehrwald, N.M., Thompson, L.G., Yao, T., Mosley Thompson, E., Schotterer, U., Alfimov, V., et al., 2008. Mass loss on Himalayan glacier endangers water resources. Geophys. Res. Lett. 35 (22), 113–130.

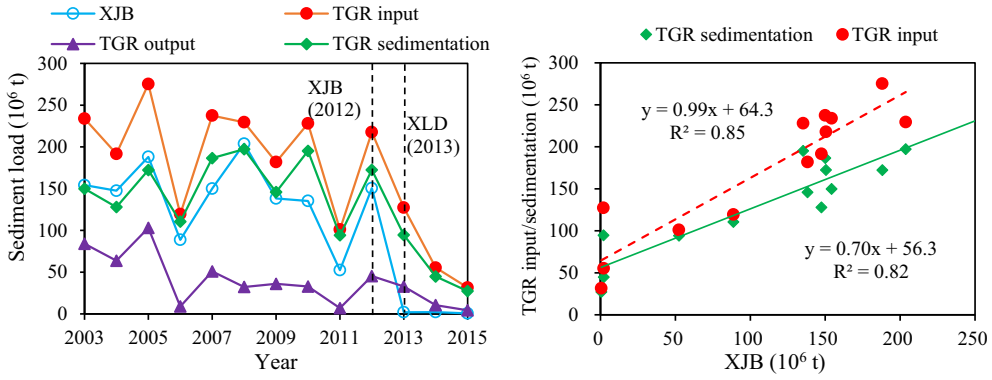

Fig. 10. Sediment load changes at the XJB station, TGR sediment input, TGR sediment output and TGR's sedimentation rate since 2003 (a) and the correlations between sediment load at the XJB and TGR sedimentation/(sediment) input (b).

Kendall, M.G., 1975. Rank Correlation Methods. Charles Griffin, London, UK.
Kummu, M., Lu, X.X., Wang, J.J., Varis, O., 2010. Basin-wide sediment trapping efficiency of emerging reservoirs along the Mekong. Geomorphology 119 (3), 181–197.
Latrubesse, E.M., Arima, E.Y., Dunne, T., Park, E., Baker, V.R., D Horta, F.M., et al., 2017. Damming the rivers of the Amazon basin. Nature 546 (7658), 363–369.
Li, Z., Xu, X., Yu, B., Xu, C., Liu, M., Wang, K., 2016. Quantifying the impacts of climate and human activities on water and sediment discharge in a karst region of Southwest China. J. Hydrol. 542, 836–849.
Liu, F., Yang, Q., Chen, S., Luo, Z., Yuan, F., Wang, R., 2014. Temporal and spatial variability of sediment flux into the sea from the three largest rivers in China. J. Asian Earth Sci. 87, 102–115.
Lu, X.X., 2005. Spatial variability and temporal change of water discharge and sediment flux in the Lower Jinsha tributary: impact of environmental changes. River Res. Appl. 21 (2–3), 229–243.
Lu, X.X., Higgitt, D.L., 1998. Recent changes of sediment yield in the Upper Yangtze, China. Environ. Manag. 22 (5), 697–709.
Lu, X., Zhang, S., Jiang, T., Xiong, M., 2010. Sediment loads in the lower Jinshajiang of the Yangtze River: current status and potential impacts of the cascade dams. IAHS AISH Publ. 337, 113–120.
Lu, X.X., Ran, L.S., Liu, S., Jiang, T., Zhang, S.R., Wang, J.J., 2013. Sediment loads response to climate change: a preliminary study of eight large Chinese rivers. Int. J. Sediment Res. 28 (1), 1–14.
Lutz, A.F., Immerzeel, W.W., Shrestha, A.B., Bierkens, M.F.P., 2014. Consistent increase in High Asia's runoff due to increasing glacier melt and precipitation. Nat. Clim. Chang. 4 (7), 587–592.
Mann, H.B., 1945. Nonparametric tests against trend. Econometrica 13 (3), 245–259.
Meade, R.H., Moody, J.A., 2009. Causes for the decline of suspended-sediment discharge in the Mississippi River system, 1940–2007. Hydrol. Process. 24 (1), 35–49.
Miao, C., Ni, J., Borthwick, A.G.L., Yang, L., 2011. A preliminary estimate of human and natural contributions to the changes in water discharge and sediment load in the Yellow River. Glob. Planet. Chang. 76 (3–4), 196–205.
Milliman, J.D., Farnsworth, K.L., 2011. River Discharge to the Coastal Ocean: A Global Synthesis. Cambridge University Press, Cambridge, p. 384.
Milliman, J.D., Farnsworth, K.L., Jones, P.D., Xu, K.H., Smith, L.C., 2008. Climatic and anthropogenic factors affecting river discharge to the global ocean, 1951–2000. Glob. Planet. Chang. 62 (3–4), 187–194.
Naik, P.K., Jay, D.A., 2011. Distinguishing human and climate influences on the Columbia River: changes in mean flow and sediment transport. J. Hydrol. 404 (3–4), 259–277.
Nearing, M.A., Jetten, V., Baffaut, C., Cerdan, O., Couturier, A., Hernandez, M., et al., 2005. Modeling response of soil erosion and runoff to changes in precipitation and cover. Catena 61 (2–3), 131–154.
Ran, L., Wang, S., Fan, X., 2010. Channel change at Toudaoguai Station and its responses to the operation of upstream reservoirs in the upper Yellow River. J. Geogr. Sci. 20 (2), 231–247.
Restrepo, J.D., Syvitski, J.P.M., 2006. Assessing the effect of natural controls and land use change on sediment yield in a major Andean River: the Magdalena Drainage Basin, Colombia. Ambio 35 (2), 65.
Syvitski, J.P., Vörösmarty, C.J., Kettner, A.J., Green, P., 2005. Impact of humans on the flux of terrestrial sediment to the global coastal ocean. Science 308 (5720), 376.
Tao, H., Gemmer, M., Bai, Y., Su, B., Mao, W., 2011. Trends of streamflow in the Tarim River Basin during the past 50 years: human impact or climate change? J. Hydrol. 400 (1–2), 1–9.
Thiessen, A.H., 1911. Precipitation averages for large areas. Mon. Weather Rev. 39 (7), 1082–1084.
Walling, D.E., 2006. Human impact on land-ocean sediment transfer by the world's rivers. Geomorphology 79 (3–4), 192–216.
Wang, H., Yang, Z., Wang, Y., Saito, Y., Liu, J.P., 2008. Reconstruction of sediment flux from the Changjiang (Yangtze River) to the sea since the 1860s. J. Hydrol. 349 (3–4), 318–332.
Wang, G., Xia, J., Chen, J., 2009. Quantification of effects of climate variations and human activities on runoff by a monthly water balance model: a case study of the Chaobai River basin in northern China. Water Resour. Res. 45 (7).
Xiong, M., Xu, Q., Yuan, J., 2009. Analysis of multi-factors affecting sediment load in the Three Gorges Reservoir. Quat. Int. 208 (1–2), 76–84.
Xu, K., Milliman, J.D., 2009. Seasonal variations of sediment discharge from the Yangtze River before and after impoundment of the Three Gorges Dam. Geomorphology 104 (3–4), 276–283.
Xu, X., Liu, W., Rafique, R., Wang, K., 2013. Revisiting continental U.S. hydrologic change in the latter half of the 20th century. Water Resour. Manag. 27 (12), 4337–4348.
Yang, X.K., Lu, X.X., 2014. Estimate of cumulative sediment trapping by multiple reservoirs in large river basins: an example of the Yangtze River basin. Geomorphology 227, 49–59.
Yang, X.K., Lu, X.X., 2015. Drastic change in China's lakes and reservoirs over the past decades. Sci. Rep. 4, 6041.
Yang, G., Chen, Z., Yu, F., Wang, Z., Zhao, Y., Wang, Z., 2007. Sediment rating parameters and their implications: Yangtze River, China. Geomorphology 85 (3–4), 166–175.
Yang, S.L., Milliman, J.D., Xu, K.H., Deng, B., Zhang, X.Y., Luo, X.X., 2014. Downstream sedimentary and geomorphic impacts of the Three Gorges Dam on the Yangtze River. Earth Sci. Rev. 138, 469–486.
Yuan, W., Yin, D., Finlayson, B., Chen, Z., 2012. Assessing the potential for change in the middle Yangtze River channel following impoundment of the Three Gorges Dam. Geomorphology 147, 27–34.
Zhang, S.R., Lu, X.X., 2009. Hydrological responses to precipitation variation and diverse human activities in a mountainous tributary of the lower Xijiang, China. Catena 77 (2), 130–142.
Zhang, Y., Liu, S., Xu, J., Shangguan, D., 2008. Glacier change and glacier runoff variation in the Tuotuo River basin, the source region of Yangtze River in western China. Environ. Geol. 56 (1), 59–68.
Zhang, M., Wei, X., Sun, P., Liu, S., 2012a. The effect of forest harvesting and climatic variability on runoff in a large watershed: the case study in the Upper Minjiang River of Yangtze River basin. J. Hydrol. 464-465, 1–11.
Zhang, N., He, H.M., Zhang, S.F., Jiang, X.H., Xia, Z.Q., Huang, F., 2012b. Influence of reservoir operation in the upper reaches of the Yangtze River (China) on the inflow and outflow regime of the TGR-based on the improved SWAT model. Water Resour. Manag. 26 (3), 691–705.
Zhao, G., Tian, P., Mu, X., Jiao, J., Wang, F., Gao, P., 2014. Quantifying the impact of climate variability and human activities on streamflow in the middle reaches of the Yellow River basin, China. J. Hydrol. 519, 387–398.
Zhao, Y., Zou, X., Gao, J., Xu, X., Wang, C., Tang, D., et al., 2015. Quantifying the anthropogenic and climatic contributions to changes in water discharge and sediment load into the sea: a case study of the Yangtze River, China. Sci. Total Environ. 536, 803–812.
Zhao, Y., Zou, X., Liu, Q., Yao, Y., Li, Y., Wu, X., et al., 2017. Assessing natural and anthropogenic influences on water discharge and sediment load in the Yangtze River, China. Sci. Total Environ. 607-608, 920–932.
Zhao, G., Mu, X., Jiao, J., Gao, P., Sun, W., Li, E., Wei, Y., Huang, J., 2018. Assessing response of sediment load variation to climate change and human activities with six different approaches. Sci. Total Environ. 639, 773–784.
Zhou, P., Luukkanen, O., Tokola, T., Nieminen, J., 2008. Effect of vegetation cover on soil erosion in a mountainous watershed. Catena 75 (3), 319–325.
Zhu, L.L., Chen, C.H., Zhang, J.S., 2016. Study on variations of runoff and sediment and effect to the lower Jinsha river. J. Sediment. Res. 5, 20–27 (in Chinese).